Anomaly detection for large span bridges during operational phase using structural health monitoring data

Author 1
Xiang Xu, PhD
School of Transportation, Southeast University, China; Key Laboratory of Safety and Risk Management on Transport Infrastructure, Ministry of Transport, China; Department of Civil and Environmental Engineering, the Hong Kong Polytechnic University, HK
230159211@seu.edu.cn

Author 2
Yuan Ren, Assistant Professor
School of Transportation, Southeast University, China; Key Laboratory of Safety and Risk Management on Transport Infrastructure, Ministry of Transport, China; Department of Civil and Environmental Engineering, University of California Irvine, USA
magren@126.com

Author 3
Qiao Huang, Professor
School of Transportation, Southeast University, China; Key Laboratory of Safety and Risk Management on Transport Infrastructure, Ministry of Transport, China

Author 4
Zi-Yuan Fan, PhD Candidate
School of Transportation, Southeast University, China; Key Laboratory of Safety and Risk Management on Transport Infrastructure, Ministry of Transport, China

Author 5
Zhao-Jie Tong, PhD
Shenzhen Municipal Design and Research Institute Co., Ltd., China

Author 6
Wei-Jie Chang
Zhejiang Zhoushan Bridge Co., Ltd., China

Author 7
Bin Liu, Lecturer
Department of Management Science, University of Strathclyde, Glasgow G1 1XQ, UK

*Corresponding to Dr. Yuan Ren (magren@126.com)

Anomaly detection for large span bridges during operational phase using structural health monitoring data

Abstract

In view of the limitation of damage detection in practical applications for large scale civil structures, a practical method for anomaly detection is developed. Within the anomaly detection framework, wavelet transform and generalized Pareto distribution are adopted for data processing. In detail, to reduce the influence of thermal responses on signal fluctuations induced by anomaly events, wavelet transform is employed to separate thermal effects from raw signals based on the distinguished frequency bandwidths. Subsequently, a two-level anomaly detection method is proposed, *i.e.*, threshold-based anomaly detection and anomaly trend detection. For the threshold-based anomaly detection, the threshold for anomaly detection is determined by generalized Pareto distribution analytics, corresponding to a 95% guarantee rate within 100 years. Moreover, the threshold is periodically updated by incorporating the latest monitoring data to model the increase of traffic volumes and gradual degradations of structures. For the anomaly trend detection, the moving fast Fourier transform is adopted for discussion. Finally, the mid-span deflection of Xihoumen Suspension Bridge is selected as the index to validate the effectiveness of the proposed methodology. Two types of anomaly events are assumed in the case study, *i.e.*, the overloading event and structural damage. The two-level anomaly detection is implemented. It is indicated through the case study that the proposed anomaly detection approach (without the influence of temperature) is able to detect three 100-ton overloaded vehicles and damages in main cables. However, the assumed cases subject to 100-ton vehicle and damages in stiffening girders are hardly detected by using the deflection index, owing to the sensitivity of the index to each anomaly event. In the future studies, a structural health monitoring-based multi-index anomaly detection system is promising to ensure the operational and structural safety of large span bridges.

Key words: large span bridges; structural health monitoring; anomaly detection; wavelet transform; generalized Pareto distribution, moving fast Fourier transform

1. Introduction

Large span bridges are usually in the critical locations within the modern traffic networks, which play a key role in regional economic development [1-3]. Meanwhile, these bridges are facing diverse threats resulting from their own structural failures and aggressive operational environments [4-6]. Owing to the scale of large span bridge structures as well as the concealment of threats, anomaly detection is a crucial task for large-scale civil structures. For instance, the I-35W bridge over the Mississippi River in Minneapolis, Minnesota, collapsed suddenly on August 1st, 2007, as a result of inadequate thickness of the gusset plates and high mean stress [7]. Thus, it is of critically importance to study practical anomaly detection methodology for large span bridges to ensure a safe operation.

In view of the availability of robust and inexpensive remote sensing technologies, structural health monitoring (SHM) systems are frequently devised to monitor bridge performance and provide real-time condition screening [8-11]. In China, almost all the large span cable-supported bridges are equipped with SHM systems. The abundant monitoring data provide solid foundation for the investigations of anomaly detection.

Damage detection has been broadly studied over the past few decades. Vibration-based damage detection is one of the most popular techniques, where the basic principle is that damages within the structure will impact the structural dynamic parameters (*e.g.*, frequency) derived from vibration monitoring data [12, 13]. In

general, the vibration-based methods are divided into two categories, namely, tradition-type and modern-type [14]. The tradition-type is mainly based on the structural vibration characteristics such as variation of natural frequencies or mode shapes [15-18]. The modern-type makes use of signal-processing techniques or artificial intelligence, including wavelet-based approaches, neural networks, *etc*. [19-23]. Cross *et al*. [24] introduced the concept of cointegration, a tool for analytics of non-stationary time series, as a promising approach for damage detection by using the index of frequency. Although vibration-based damage detection methodology has been successfully applied to mechanical and aerospace engineering fields, challenges still exist in civil engineering since dynamic parameters are significantly influenced by noise, environmental variations, *etc*. Changeable operating environments (*e.g*., temperature) introduce problems to the research of structural damage detection, especially for large scale structures. Xu and Wu [25] proved that changes in dynamic characteristics due to temperature may be greater than that induced by damages. Peeters *et al*. [26] also emphasized the importance in distinguishing the temperature effects from real damage events.

Considering the limitation of vibration-based damage detection methods, researchers explored static-based characteristics for structural damage detection. Posenato *et al*. [27] took advantages of strains to detect damages using two statistical methods, *i.e*., moving principal component analysis and robust regression analysis. Wu *et al*. [28] presented a damage detection method for concrete continuous girders using spatially-distributed long-gauge strain sensing. Chen *et al.* [29] proposed an effective method for structural damage detection based on the measurements of stay cable force and structural temperatures. Yu *et al.* [30] applied the continuous wavelet transformation to process deflection data for damage detection. Zhu *et al*. [31] presented a temperature-driven moving principle component analysis method using strain measurements to detect structural anomalies. Similar to the vibration-based damage detection, environmental factors also weaken the effectiveness of the static-based approach. Yarnold and Moon [32] developed a damage detection method considering the influence of temperature, where the measurements of strain and displacement were used for discussion. Compared with the vibration-based SHM approach, the results indicated that the temperature-based approach was more sensitive for the events examined. Kromanis and Kripakaran [33] proposed a regression-based methodology to generate numerical models between distributed temperatures and responses collected during a reference period, which will support evaluation of bridge response to diurnal and seasonal changes in environmental conditions. Zhu *et al*. [34] presented a feature extraction method to uncover the temperature effects on girder strains, which combined mode decomposition, data reduction, and blind source separation. Xu *et al.* [35] proposed a practical multivariate linear-based model for modelling and separation of thermal response from the girder deflection monitoring data. Ren *et al.* [36] used regression analysis to simulate the thermal effects within cable force measurements of a cable-stayed bridge.

Considering the complicacy of bridge structures and harsh environments, there is still a substantial gap for both vibration- and static-based damage detection methodologies when applied in practical engineering. In this regard, the gap includes (1) indexes for damage detection may be significantly contaminated by noise; (2) signal fluctuation induced by structural damages may be covered by that due to environmental factors (*e.g.*, temperature); (3) indexes for damage detection may not be much sensitive to localized damages; and (4) anomalous signals may result from those anomaly events rather than structural damage. Zong *et al.* [37] concluded that the structural damage detection techniques based on SHM measurements are mostly at the stage of laboratory, and difficult to realize the early damage detection for large span bridges.

Considering the requirements of engineering applications, this paper explores to extend damage detection

to anomaly detection. The objective of anomaly detection is to find patterns in dataset that do not confirm to the expected behaviors [38]. These nonconforming patterns may result from instant damages or accidents during operation stages. For instance, the anomaly event could be overloaded vehicles passing through the bridge, in addition to structural damages. As discussed earlier, thermal effects act as a hindrance for data interpretation. Wavelet transform is used to separate thermal effects from the raw monitoring signals based on the periodicity of temperature loads. Based on the training dataset corresponding to normal operational scenarios, the threshold for anomaly detection is determined by using generalized Pareto distribution (GPD) analytics. Furthermore, the energy-based method for anomaly trend detection is proposed by using moving fast Fourier transform (MFFT). Aiming to validate the effectiveness of the proposed methodology, a numerical model is created, and 5 cases (*i.e.*, 3 anomaly events and 2 structural damage cases) are simulated on it.

2. Methodology

The general flowchart of the anomaly detection methodology in this paper is shown in Fig. 1. Raw signals from SHM systems are first pre-processed, including de-noising, gross error detection and missing data imputation. The pre-processing procedure could refer to our previous work [8]. Subsequently, thermal response separation is implemented to obtain qualified signals for the following discussion. Finally, a 2-level anomaly detection is carried out. For the first level anomaly detection (*i.e.*, threshold-based anomaly detection), GPD is used to determine the threshold based on the training dataset subject to normal behaviors. Moreover, the threshold is updated with the latest monitoring data to model the increase of traffic volumes and gradual structural degradations. For the second level anomaly detection (anomaly trend detection), the MFFT is adopted to obtain the time and frequency domain information.

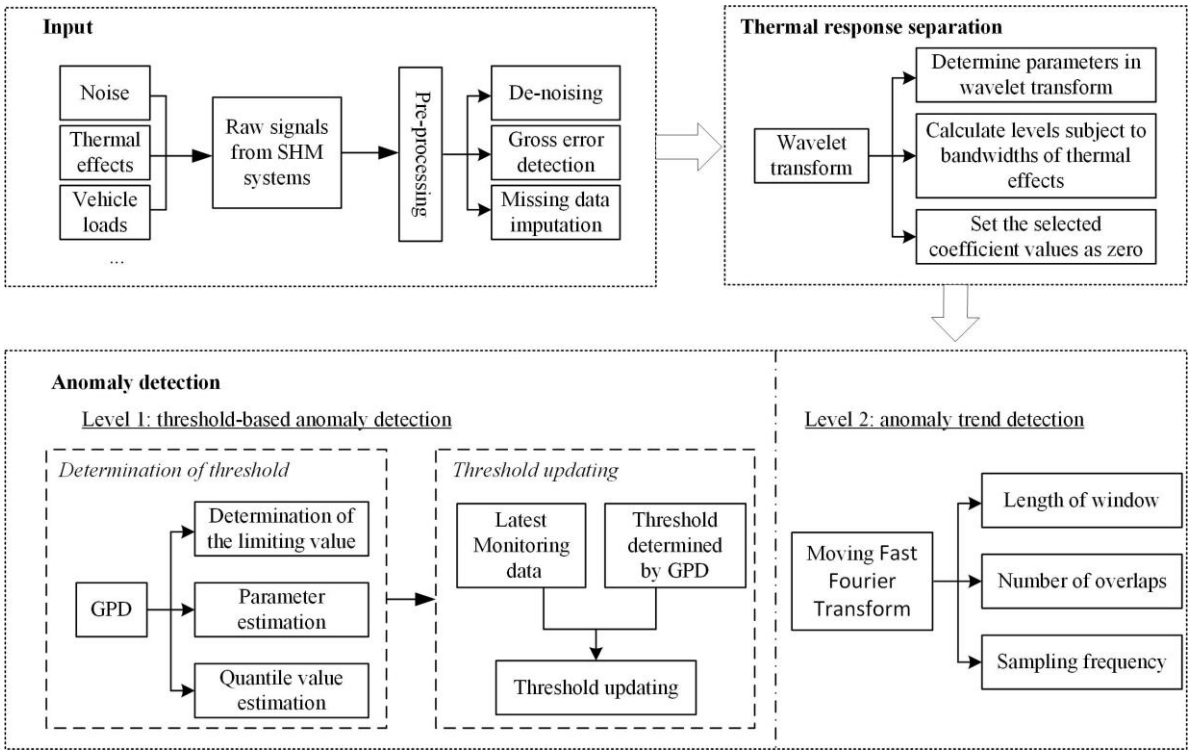

Fig. 1 Outline of the methodology

2.1 Thermal response separation

Methods regarding thermal response modelling have been well studied in recent years [39-43]. The wavelet

transform technique is one of the most popular tools in this research area.

The wavelet transform is developed from the Fourier transform. Compared with the Fourier transform, the wavelet transform has advantages in analyzing local characteristics both in time and frequency domain, and dealing with non-stationary signals. The continuous wavelet transform of a time-domain signal $f(t)$ is expressed as

$$W_f^{\psi}(a,b) = \frac{1}{\sqrt{a}} \int_{-\infty}^{+\infty} f(t) \psi\left(\frac{t-b}{a}\right) dt \tag{1}$$

where *a* and *b* are scaling and shift parameters of the wavelet function $\psi(t)$, respectively. However, the discrete wavelet transform is much more frequently applied in engineering applications, which is given as

$$W_f^{\psi}(j,k) = 2^{-j/2} \sum_n f(n) \psi\left(2^{-j} n - k\right) \tag{2}$$

where $f(n)$ is a discrete sequence, $\psi(n)$ the wavelet function, and $2^{(-j/2)} \psi\left(2^{-j} n - k\right)$ are scaled and shifted versions of $\psi(n)$ with values of *j* (scaling coefficient) and *k* (shifting coefficient).

Combination of the discrete wavelet transform and filters (*i.e.*, wavelet-based multi-resolution analysis) is able to decompose signals into various resolution scales. The data with coarse resolution, termed as approximations, contain information regarding low frequency components and retain the main features of raw signals, while the data with fine resolution (*i.e.*, details) retain information of the high frequency components and reflect detailed features of the original signals. The approximation signal $A_j(n)$ at the j^{th} resolution level is computed as

$$A_j(n) = \sum_{k=-\infty}^{\infty} a_{j,k} \phi_{j,k}(n) \tag{3}$$

where $a_{j,k}$ is the approximation coefficient, and $\phi_{j,k}$ is called the scaling function. The detail signal $D_j(n)$ is then demonstrated as

$$D_j(n) = \sum_{k=-\infty}^{\infty} d_{j,k} \psi_{j,k}(n) \tag{4}$$

where $d_{j,k}$ is the detail coefficient, and $\psi_{j,k}$ is the wavelet basis function. The original signal can be reconstructed using the approximation at the M^{th} resolution level and all the details starting from the first level until the M^{th} level, which is

$$x(n) = \sum_{k=-\infty}^{\infty} a_{M,k} . \phi_{M,k}(n) + \sum_{j=1}^{M} \sum_{k=-\infty}^{\infty} d_{j,k} \psi_{j,k}(n) \tag{5}$$

The first term represents the approximation at level *M* and the second term represents the details at and below level *M*. A schematic representation of the wavelet-based multi-resolution analysis pyramid structure is shown

in Fig. 2.

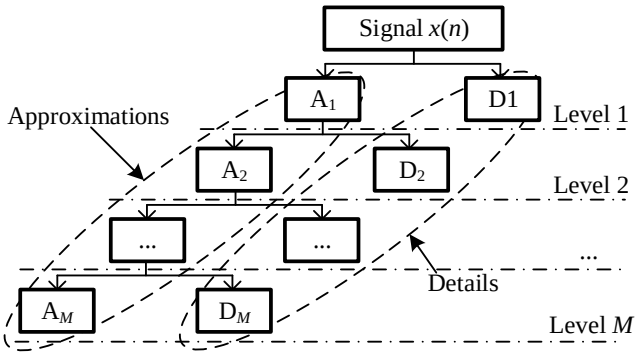

Fig. 2 Pyramid structure of the wavelet-based multi-resolution analysis

Thermal actions have substantial periodicity, including the period of 24 hours for diurnal thermal actions and the period of 1 year for seasonal thermal actions [44, 45]. Thus, both the two types of thermal effects are supposed to be confined within a specific bandwidth in frequency domain. Based on the definition of the wavelet transform, each signal decomposition corresponds to a certain bandwidth. Therefore, thermal response separation is realized by calculating the level corresponding to the bandwidth of thermal effects, then setting the coefficient values of the determined signal decompositions as zero at reconstruction.

2.2 Threshold-based anomaly detection

2.2.1 Determination of threshold

To realize quasi-static anomaly detection, it is required to consider the responses from all known loads (*e.g.*, temperature loads, traffic loads and so on) [46]. In view of the complicacy of operating conditions for large span bridges, the existing technology cannot identify the space-time distribution of vehicle loads effectively. It is difficult to separate responses due to random vehicle loadings from the monitoring data. Thus, vehicle loadings are treated as random variables in this paper, which are addressed by using the statistical method. It is assumed that under normal operation scenarios, the response of vehicle loadings within a certain time window satisfies the distribution of determined statistical parameters (*i.e.*, mean and variance). The structural anomaly detection is based on the rationale that when an anomaly event occurs during operation stages, the monitoring value of its structural response will substantially exceed the normal range. Thus, anomaly detection in structural analysis is simplified to outlier identification in digital signal processing.

In general, the anomalous data are defined as those signals outside the threshold. Extreme value analysis (EVA) is widely used to predict the threshold. For example, Liu *et al*. [47] took advantages of the EVA to determine the extreme deflection values for condition evaluation of suspension bridges. The EVA is a supplement to the normal distribution, which is used to model the tail data of the normal distribution.

The block maximum method is a typical EVA method in practical applications [48]. The block maximum model is built up by 3 steps: (1) dividing all observations into k groups on average; (2) extracting the maximum value in each group for discussion; and (3) performing distribution analysis using the extracted maximum data. However, the block maximum model only focuses on the largest data and ignores the remaining data in the group. Considering that the block maximum model cannot make full use of the extreme value information, the Pareto distribution analysis is adopted to determine the threshold for structural anomaly

detection. The Pareto distribution analysis takes advantages of data that are larger than a defined limiting value.

If the distribution function of the random variable **X** is

$$G(x;\mu,\sigma,\zeta)=\begin{cases}1-\left(1+\zeta\dfrac{x-\mu}{\sigma}\right)^{-1/\zeta}, & \zeta\neq 0\\ 1-\exp\left(-\dfrac{x-\mu}{\sigma}\right), & \zeta=0\end{cases} \tag{6}$$

then, it is called that variable **X** obeys GPD, where the support is $\frac{x-\mu}{\sigma}\geq 0$ for $\zeta\geq 0$ and $0\leq\frac{x-\mu}{\sigma}\leq -1/\zeta$ for $\zeta<0$, μ is the position parameter, σ the scale parameter, and ζ the shape parameter.

The regular steps to determine the quantile estimates at *T*-year return period are as follows:

(1) Determination of the limiting value. When Pareto distribution is used to fit the excess quantity, it is a critical challenge to determine the limiting value. If the limiting value is high, the number of out-of-sample is small resulting in a severe variance of estimators; on the other hand, if the limiting value is low, the excess quantity differs significantly from the GPD leading to a biased estimator. The average excess function $e(u)$ of the GPD is a linear function of the excess quantity u. For a given sample, the average excess function of the sample greater than the limiting value should fluctuate around a straight line. The limiting value can be determined by focusing on the slope change characteristics of $e(u)$ after a certain limiting value u_0. The point where the slope remains constant can be used as the limiting value.

(2) Parameter estimation. Based on the existing sample data, the parameters of the GPD model are estimated. The common estimation methods include maximum likelihood estimation, probability moment estimation, *L* moment method.

(3) Quantile value estimation. Within a *T*-year return period, the quantile p corresponding to a certain guarantee rate *Pr* is

$$p=1-\sqrt[T]{\Pr} \tag{7}$$

The corresponding quantile value x_p is

$$x_p=u_0+\frac{\hat{\sigma}}{\hat{\zeta}}\left[\left(\frac{n}{N_u}(1-p)\right)^{-\zeta}-1\right] \tag{8}$$

where $\hat{\sigma}$ is the scale parameter estimate, $\hat{\zeta}$ the shape parameter estimate, n the number of samples, and N_u the number of data that exceed the limiting value.

According to JTG D60-2015, the design actions are defined as the quantile value corresponding to the 95% guarantee rate with a reference period of 100 years. In order to keep consistent with the design actions at the probability level, the threshold used for structural anomaly detection is defined as the quantile value corresponding to the 95% guarantee rate with a reference period of 100 years.

2.2.2 Threshold updating

With the development of social economy and travel demand, traffic volumes of bridges are bound to rise with time. Moreover, structural gradual degradations will weaken the stiffness of structures. Although maintenance

activities are implemented on these gradual degradations, the condition of the bridge can hardly resume to its initial state. The increase of both the traffic volumes and structural unrecoverable degradations will influence the level of structural response gradually. The effectiveness of anomaly detection will be significantly reduced by using lagged thresholds under current service status, which will lead to false detection. For instance, the thresholds of the girder deflection at mid-span of Xihoumen Suspension Bridge (XSB) in 2010, 2014 and 2017 are -0.463m, -0.605m and -0.811m, respectively. One could refer to the case study section for the detailed calculation process. If the threshold of deflection in 2010 (-0.463m) is used for anomaly detection in 2014, false abnormalities will be frequently detected owing to the increase of traffic volume and gradual degradations. Moreover, the frequent false detection alarming will influence the confidence of owners to the detection results. Thus, it is essential to upgrade the threshold periodically by using the latest monitoring data. The threshold updating flowchart is shown in Fig. 3. In this paper, it is suggested to annually update threshold. The specific period for threshold updating depends on the practical requirements.

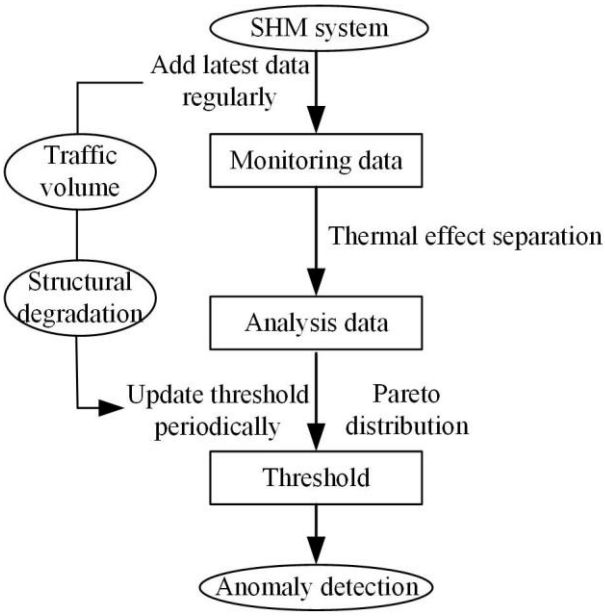

Fig. 3 Flowchart of the threshold updating

The threshold determined by using GPD is from the statistic point of view, rather than the structural safety and serviceability analytics. There exists a limit for thresholds regarding to structural serviceability concerns. For example, according to JTG/T H21-2011, the most unfavorable deflection at mid-span of a suspension bridge is 1/500*L*, where *L* is the main span length of the bridge. For the studied XSB with a main span of 1650m, the limit is calculated as 3.3m subject to structural serviceability. When the threshold determined by GPD reaches the limit defined by the code (*i.e.*, 3.3m in this study), special inspections and rehabilitations are recommended to carry out to guarantee the performance of the structure.

2.3 Anomaly trend detection

The aforementioned threshold-based anomaly detection method focuses on single measurement, which could not reflect the variation trend of the recorded signals. However, structural damages prefer to disturb the variation trend of the response. Herein, the MFFT algorithm is used to obtain the time and frequency information of the signal, which will help to detect anomaly trend of the measurements.

Considering measurements $x_0, x_1, \ldots, x_{N-1}$, and suppose that their *N*-point discrete Fourier transform (DFT)

$F(u)$, u=0,1,…,N-1 is already computed. Let the data be moved one point to the right, including the new value x_{add}. Call the new data $x_{\text{new}}(t)$, where

$$\begin{aligned} x_{new}(t) &= \begin{Bmatrix} x(t+1), t = 0,1,...,N-2 \\ x_{add}, \quad t = N-1 \end{Bmatrix} \\ &= \begin{Bmatrix} x(t+1), t = 0,1,...,N-2 \\ x_0, \quad t = N-1 \end{Bmatrix} + \delta_{t,N-1}(x_{add} - x_0) \end{aligned} \tag{9}$$

where δ is the Kronecker delta function.

The first term on the right hand side represents the N original points $x(t)$ rotated one position to the left. Taking the DFT and applying the Fourier shift theorem yields as

$$F_{new}(u) = \left[F(u) + \frac{x_{add} - x_0}{N} \right] \exp\left(j \frac{2\pi u}{N} \right), u = 0,1,...,N-1 \tag{10}$$

This formula shows how to update a one-dimensional discrete Fourier transform by including the new point x_{add} and removing the x_0.

3. Case study

3.1 Background: bridge and its monitoring system

A large span suspension bridge, the XSB, is used to illustrate the effectiveness of the proposed anomaly detection method. The XSB, a cross-sea bridge in Zhoushan city, Zhejiang Province, China, lies above Xihoumen waterway, as a part of Yongzhou Expressway. It is a suspension bridge with a main span of 1650m. The superstructure deck has a 3.5m deep and 36m wide orthotropic steel box girder that accommodates two lanes in each direction. The bridge was opened to traffic on December 25, 2009, and the design vehicle speed is limited to 80km/h.

The girder deflection at mid-span is selected as the index for structural anomaly detection. Compared with deflections at other locations (*e.g.*, 1/4L), mid-span deflection measurements are more sensitive to live loads, which is commonly used to rate the short- and long-term global behavior of long span bridges [35, 47, 49, 50]. The spatial information of main cables, steel box girders and towers are obtained by global position system (GPS). The deployment of GPS is shown in Fig. 4. There are four GPS used for girder alignment monitoring, eight GPS for main cable monitoring, and four for towers. The sampling frequency of GPS is 20Hz, and the real-time dynamic measurement accuracy in vertical direction is ±20mm+1ppm RMS, that is, the basic error of measurements is 20mm, then the accuracy decreases by 1mm for each 1km increasing in the distance between the measuring point and the base station. The alignment of the girder at bridge construction completion moment is defined as the baseline. The deflection is the vertical distance of the interested location from the baseline, where negative values mean flexural downbows, while the positive indicates bent-up.

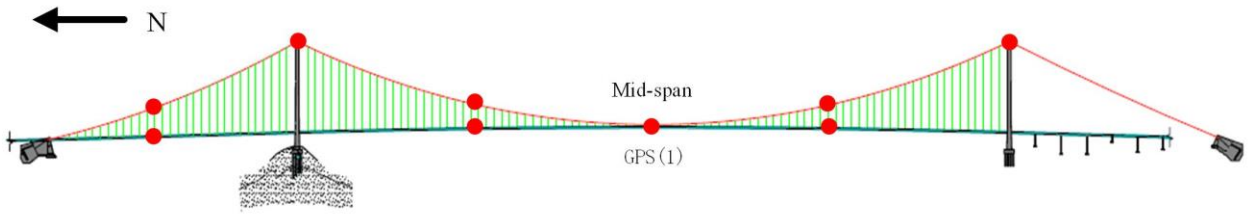

Fig. 4 Layout of GPS

3.2 Separation of thermal response

In view of the high sampling frequency of GPS (*i.e.*, 20Hz), data resampling is implemented to improve the efficiency of data processing. For anomaly detection, mean value will produce peak clipping phenomenon, leading to omission of detection. Therefore, the minimum values of the mid-span deflection (down-warping) measurements are adopted for the following discussions. Hourly minimum mid-span deflection measurements in Jan., Apr., Jul. and Oct., 2014 as well as their temperatures are shown in Fig. 5(a). Moreover, the minutely minimum mid-span deflections and ambient temperature data during Oct. 8, 9 and 10, 2014 are plotted in Fig. 5(b). The monitoring deflection data indicate significant daily and seasonal periods. With the increase of ambient temperature, the mid-span deflection goes down [51-53].

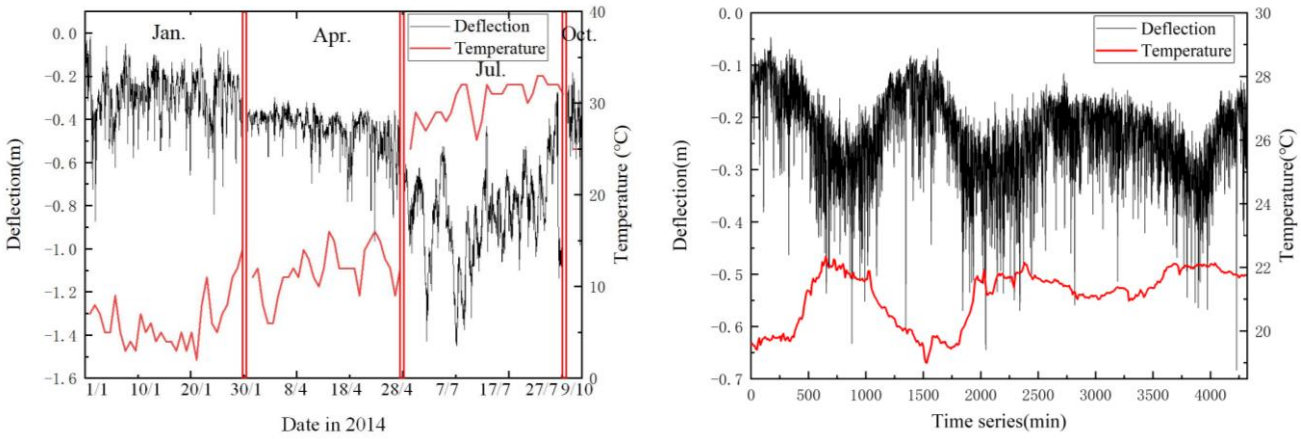

(a) Hourly minimum deflections and temperatures in four months

(b) Minutely minimum deflections and temperatures in three days

Fig. 5 Minimum deflections and temperatures in two time scales

The wavelet transform is applied to separate thermal response from the recorded measurements based on the distinguished frequency bandwidth of each signal decomposition. In general, the periods of diurnal and seasonal actions are 24 hours and 365 days, respectively. Minutely minimum deflections during three days as shown in Fig. 5(b) are taken as the example to demonstrate the wavelet-based thermal response separation process. Based on the frequency bandwidth division rule as shown in Fig. 6, the raw monitoring deflection data are decomposed into 17 levels. The energy spectrum of each detailed layer is shown in Fig. 7. The 10^{th} detail layer (D10) subject to a period of approximate 24-hour contains the largest weights of energy compared with others since the diurnal thermal response lies on the 10^{th} layer. Seasonal thermal response is recognized as the approximation signal component (A17) based on the distinguished frequency bandwidth. In detail, the decomposition (A17) contains signals whose periods are around 365 days, which fits the period of seasonal response. The wavelet basis function is set as DB8 in this case according to trials and errors. As a result, the

diurnal and seasonal sub-signals are demonstrated in Fig. 8(a) and Fig. 8(b), and the signals after thermal response separation are shown in Fig. 8(c).

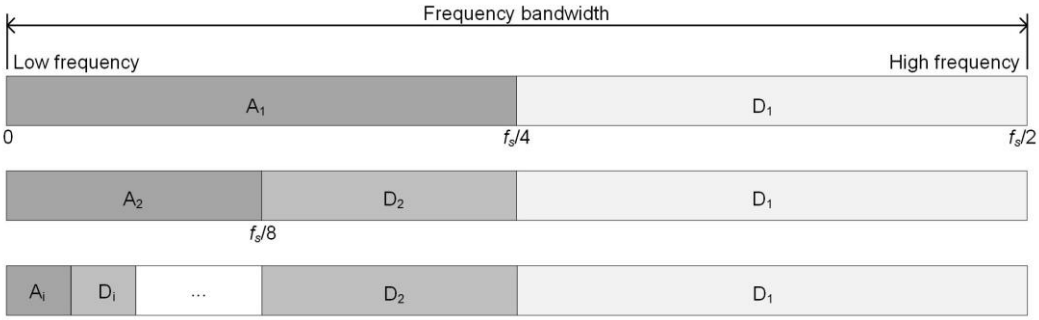

- where f_s is the sampling frequency.

Fig. 6 Frequency bandwidth division rule

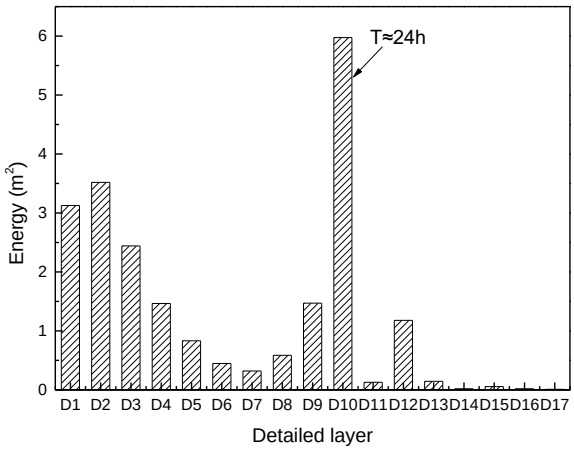

Fig. 7 Energy spectrum of each detailed layer

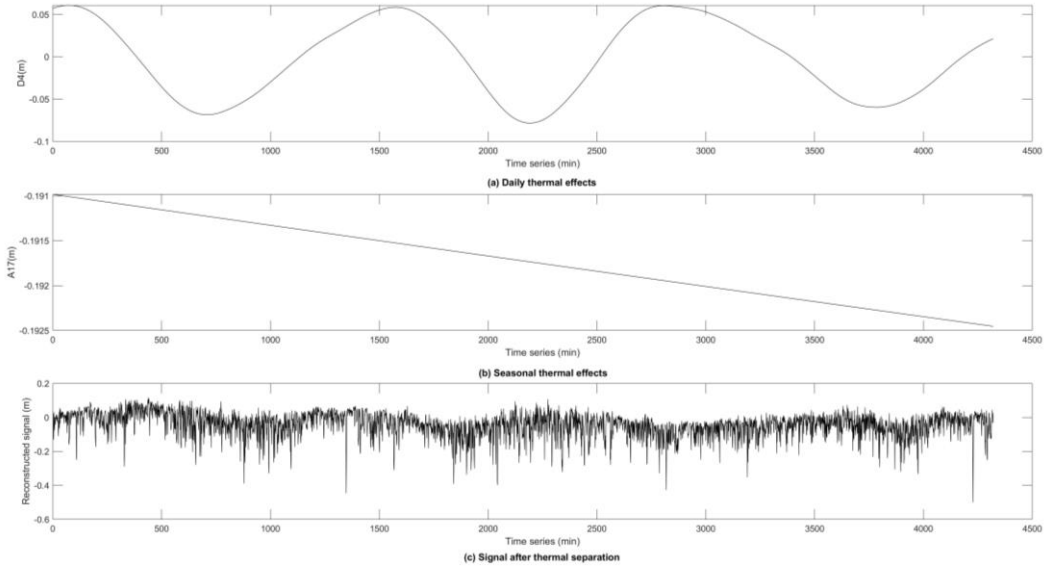

Fig. 8 Typical sub-signal after wavelet transform

Hourly minimum deflection measurements in Jan., Apr., Jul. and Oct., 2014 (as shown in Fig. 5(a)) are processed by using the wavelet transform. The resampling frequency is 1/3600Hz. The reconstructed signals are shown in Fig. 9, excluding the effects of thermal actions.

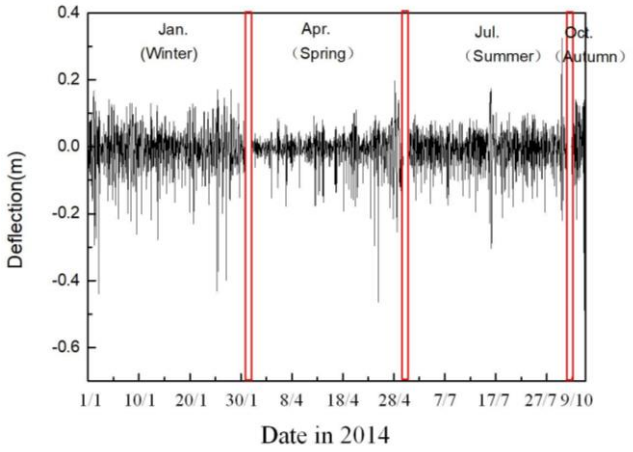

Fig. 9 Thermal response separation for seasonal monitoring data

3.3 Determination of threshold

After obtaining the reconstructed signals, the GPD is applied to determine the threshold for anomaly detection. According to the definition of the Pareto distribution, only the data smaller than the limiting value (in this case) are used for the following discussion. The first step is to determine the limiting value. The relationship between the mean excess quantity and the limiting value is shown in Fig. 10. Based on the rule that the average excess function of the sample smaller than the limiting value should fluctuate around a straight line, the limiting value is set as -0.02m in this case. The reconstructed deflection data smaller than -0.02m are used for GPD fitting analysis. The estimated shape parameter and scale parameter are $\hat{\zeta}$=-0.0993 and $\hat{\sigma}$=0.0795, respectively, which are calculated by MATLAB platform by using the maximum likelihood estimation. With the determined shape and scale parameters, the probability density function is shown in Fig. 11. Considering the reference period of the bridge (100 years), the threshold of the mid-span deflection is -0.605m according to Eq. (8), which corresponds to 95% guarantee rate within 100 years.

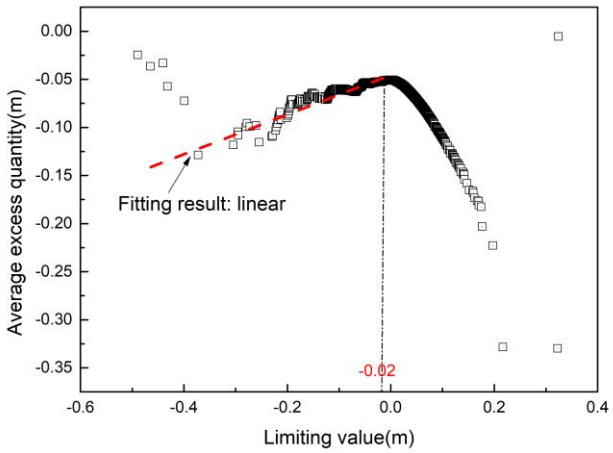

Fig. 10 Relationship between the mean excess quantity and the limiting value

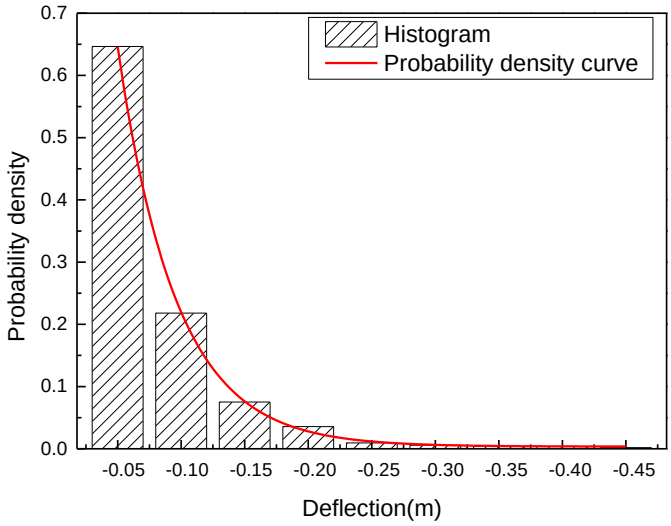

Fig. 11 Probability density function

3.4 Threshold updating

With the advance of social economy, the traffic volume is constantly increasing, intensifying the stiffening girder under-warping. Moreover, structural gradual degradations will weaken the stiffness of the girder, leading to larger deformations. In all, the threshold derived from the GPD will vary with time. Thus, it is urgent to update the threshold with the latest monitoring data to ensure the effectiveness of the proposed structural anomaly detection.

Following the steps of GPD analytics, the thresholds of the mid-span deflection in 2010, 2014 and 2017 are calculated and listed in Table 1. With the increase of the traffic volume and decrease of the girder stiffness, the absolute value of mid-span deflection increases with the time. However, the thresholds in the three years are all far smaller than the limit value 3.3m. Therefore, the monitoring deflections under normal operation conditions are way smaller than the limit, which indicate that current monitoring deflections will not influence the serviceability of the bridge.

Table 1 Thresholds of the mid-span deflection in 2010, 2014, and 2017

Year	Threshold (m)
2010	-0.463
2014	-0.605
2017	-0.811

3.5 Result discussion

3.5.1 Threshold updating

Aiming to highlight the necessity of threshold updating, the threshold calculated by deflection data in 2010 is used for structural anomaly detection in 2014. The sampling data in Fig. 12 are monitored by GPS under normal bridge operating state in 2014. For the mid-span deflection measurements in 2014, two detections occur when using the threshold in 2010 (-0.463m) as shown in Fig. 12. In fact, no anomaly events were observed at the detection instants, which indicates false alarms. The false detections are mainly caused by the

increase of traffic volumes between 2010 and 2014, which enhances the magnitude of the mid-span deflection. When the threshold in 2014 is employed, no false detection is observed. Thus, threshold updating could avoid false detection to enhance the effectiveness of the proposed anomaly detection approach.

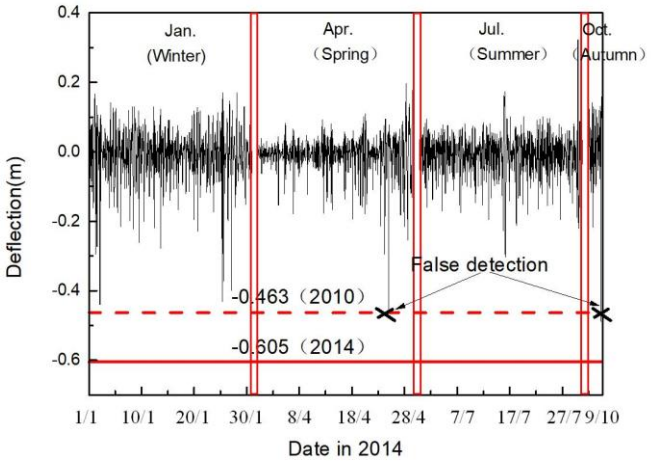

Fig. 12 Detection results by using threshold in 2010 and 2014

3.5.2 Overloading detection

To demonstrate the advantages of the proposed detection methodology, anomaly detection using raw deflection signals is carried out, which is commonly applied in practical engineering. The raw deflection data involving thermal effects in 2014 are processed by using GPD directly as discussed earlier, and the calculated threshold is -1.506m in this case. In consideration of the difficulty in collecting anomalous data samples, three events (*i.e.*, two anomaly events and one normal event) are simulated to validate the effectiveness of the anomaly detection method, which are

- Case 1: involving three 100-ton overloaded vehicles in the normal traffic flow at T_1, which should be detected as an anomaly event;
- Case 2: adding a standard 55-ton vehicle to the normal traffic flow at T_2, which should not be detected;
- Case 3: a 100-ton overloaded vehicle passing through the bridge at instant T_3, which is supposed to be detected.

The initial FE model for the XSB was developed on the software platform MIDAS/CIVIL 2010. Beam and truss elements were used to model the girders and cables. A total of 899 nodes and 896 elements were built up in the entire model. The model updating process was conducted to make both the dynamic and static responses in line with the actual ones. In brevity, the model updating procedure will not be introduced herein. Based on the modified finite element (FE) model of the XSB, the mid-span deflections subject to Cases 1 and 2 are obtained as shown in Fig. 13.

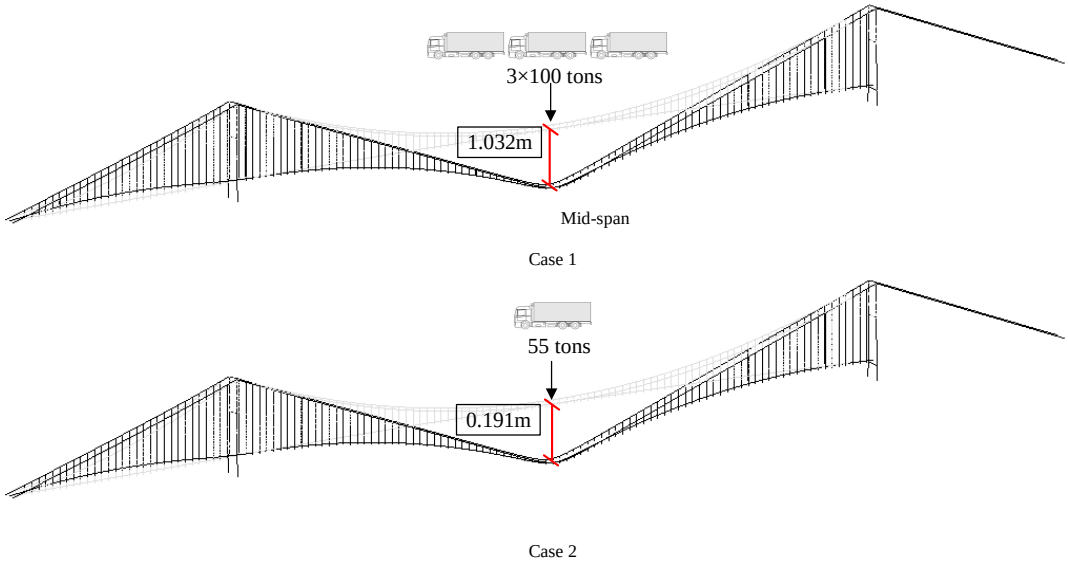

Fig. 13 Deflections under Cases 1 and 2 calculated by using the FE model

A significant gap is observed in the monitoring deflections between the winter and summer as shown in Fig. 14(a), resulting from the seasonal temperature difference. In Case 1, three 100-ton overloaded vehicles travel through the bridge simultaneously at T_1 in the winter. The response of the mid-span deflection does not reach the threshold as shown in Fig. 14(a), resulting in an omission. In Case 2, a 55-ton standard vehicle goes through the bridge at T_2 in the summer. The response of the deflection exceeds the threshold as shown in Fig. 14(a), leading to a false detection. Both the omission in the winter and false detection in the summer are attributed to the thermal effects, which are sometimes larger than the response induced by vehicle loadings and will cover the fluctuations caused by anomaly events. Thus, the effectiveness of the anomaly detection method is significantly influenced by thermal effects.

The proposed anomaly detection methodology takes advantages of structural response that is pre-processed to separate out thermal response. The detection results are shown in Fig. 14(b) by using mid-span deflection measurements in 2014. The Case 1, *i.e.*, three 100-ton overloaded vehicles travelling through the bridge simultaneously at T_1, is detected successfully to indicate the abnormal operating state, while the Case 2, *i.e.*, a 55-ton standard vehicle through the bridge at T_2, is judged as normal operating condition. Compared with the anomaly detection results derived from the raw monitoring data as shown in Fig. 14(a), the effectiveness of the anomaly detection approach has been greatly improved by separating thermal effects from the structural response.

Case 3 is simulated as a 100-ton overloaded vehicle passing through the bridge at instant T_3. The deformation of the mid-span section is 0.347m (downward) subject to the Case 3 through the FE model simulation. We fail to detect the overloading event as shown in Fig. 14(b). It is concluded that the effectiveness of the proposed overloading detection method is not only influenced by the weight of the overloaded vehicle but also the other vehicle loads on the deck simultaneously. The existence of other vehicles will introduce errors in overloading detection results.

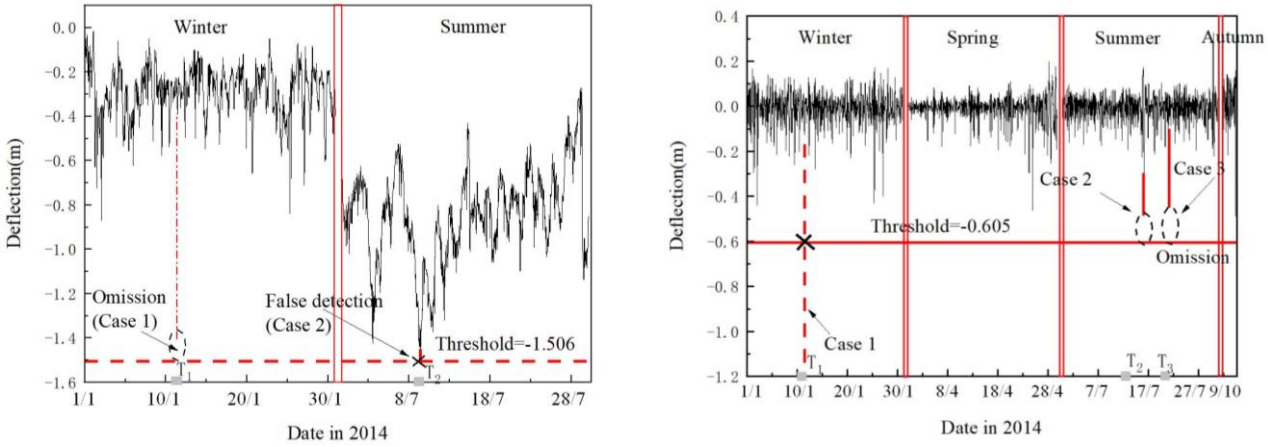

(a) Anomaly detection using raw deflection data (b) Anomaly detection using the proposed method

Fig. 14 Overloading detection results

3.5.3 Damage detection

Considering no remarkable damage occurring on the studied bridge within the service age, simulated damage events are employed. The main cable is one of the critical components in the suspension system. Meanwhile, the condition of main cables is difficult to inspect owing to the covering layer. Herein, two cases regarding structural damages are assumed as: (1) damage case 1: a 40% reduction of Young's modulus within the midspan section of the main cables; and (2) damage case 2: a 40% reduction of Young's modulus within the mid-span section of the girder.

Both the field monitoring data (Aug. 16 and 17) and FE models are used for the simulation of damage detection study. The established FE model is used to model the damaged structure with a 40% reduction of Young's modulus within the midspan section. Then, the calculation results of the FE model are integrated with the in-situ measurements at the instant *T*. Based on the threshold calculated earlier, the detection results are shown in Fig. 15(a). As a result, multiple anomalous signals are detected after the instant when damage was imported. In the overloading detection, the anomalous signals are confined into a short time window since the structure behaviors resume normal when the overloading vehicles pass away. However, there is a different signal pattern for damage detection. In detail, anomalous signals will be continuously detected in damage detections until the damage is corrected. Next, the spectrum is adopted by applying MFFT to the time histories with a window length of 128, and the spectrum energy is shown in Fig. 16(a). The energy of the signal subject to structural damage is higher than that corresponding to the sound condition. The reason is that the structural damages weaken the stiffness of the structure, resulting in larger fluctuation of deflection signals. The larger the amplitude is, the more energy the signal contains.

The other case study is conducted herein, which introduces a 40% reduction of Young's modulus within the mid-span section of the girder. The detection result is shown in Fig. 15(b), where the damage cannot be detected using the deflection. The detection index, *i.e.*, mid-span deflection, is not so sensitive to the Young's modulus of the girder compared with the main cables since the stiffness of the suspension bridge is mainly provided by main cables rather than the girder. Similarly, the spectrum energy of the signal is plotted as shown in Fig. 16(b). Similar results are drawn as shown in Fig. 15(b), omission occurred by using spectrum energy for damage detection. Based on the rationale that different parameters are sensitive to different anomaly

events, a SHM-based multi-index anomaly detection system is promising to ensure the operational and structural safety of large span bridges.

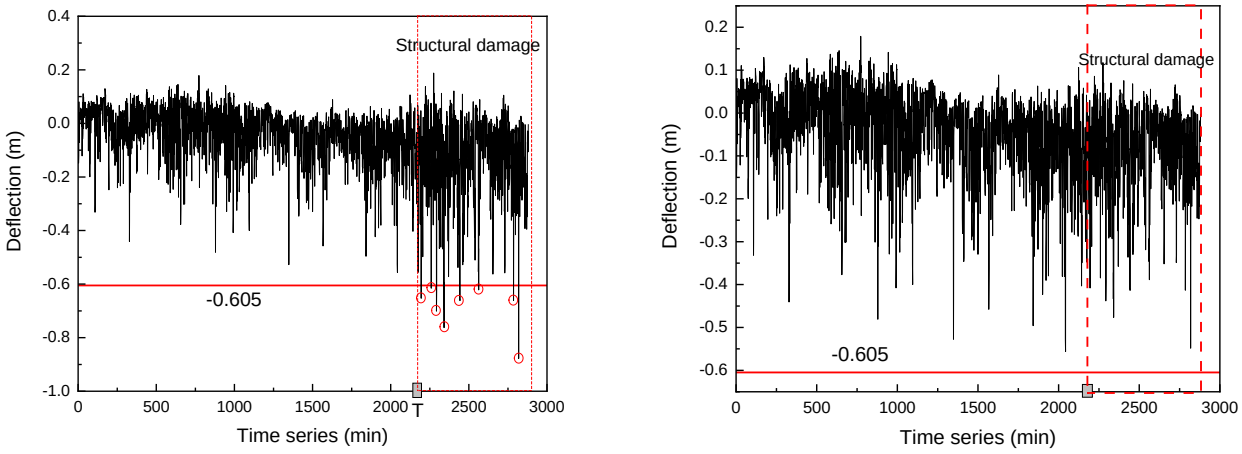

(a) Damage case 1 (b) Damage case 2

Fig. 15 Damage detection results

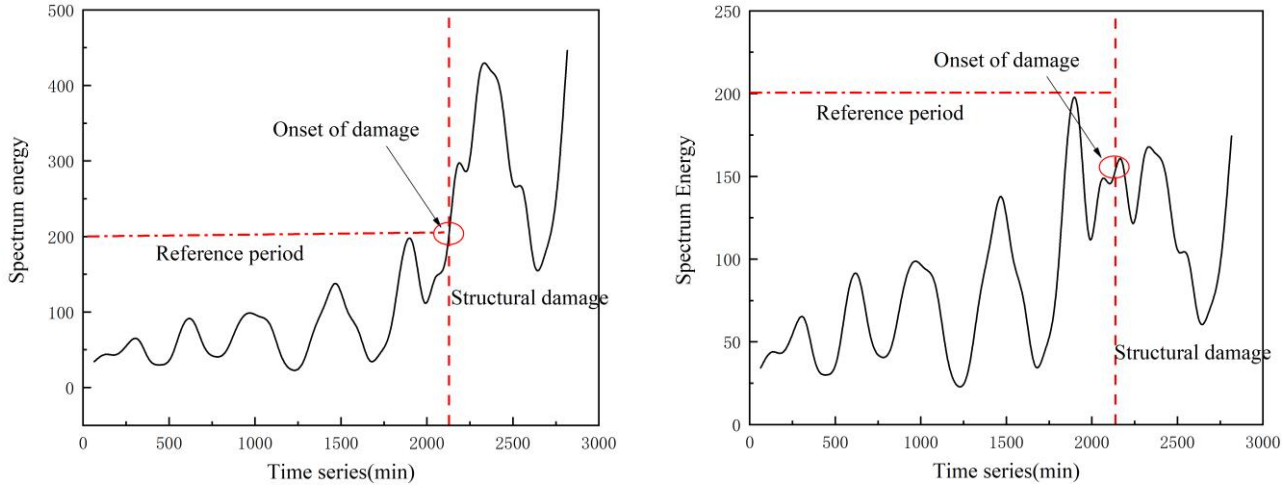

(a) Damage case 1 (b) Damage case 2

Fig. 16 Spectrum energy obtained by MFFT

The case study takes the mid-span deflection of stiffening girder of a suspension bridge as an example to verify the effectiveness of the anomaly detection method. When other structural response (*e.g.*, strain) is selected as the index, the proposed method is still applicable. However, specific discussions regarding the influence of various factors (*e.g.*, temperature, traffic volumes) to the index are necessary to ensure the accuracy and robustness of the anomaly detection method.

4. Conclusions

This paper has developed an anomaly detection method for bridges by using the wavelet transform and Pareto distribution analytics based on SHM data. The following conclusions can be drawn from this study:

(1) Wavelet transform method is applied to separate thermal effects from the raw monitoring signals. Based on the periods of diurnal thermal actions (24 hours) and seasonal thermal actions (365 days), the wavelet transform-based sub-signals corresponding to the diurnal thermal effects and seasonal ones are determined and separated from the raw monitoring signals.

(2) In view of the limitations of the block maximum method, the GPD is used to predict the threshold for structural anomaly detection. Since the design reference period of large-scale bridges is generally 100 years, the threshold is defined as the statistical value corresponding to the 95% guarantee rate within the reference period. Moreover, the threshold is required to be updated using latest monitoring data to consider the increase of traffic volumes and degradations of the structure.

(3) Deflection at mid-span of the XSB is selected as the index to validate the effectiveness of the proposed anomaly detection method by using the data generated from an FE model. The absolute value of the threshold increases with the operating time owing to the increase of the traffic volume and degradation of the structure. Through the investigations of overloading and damage detections, it is concluded that the proposed anomaly detection method considering thermal effects has more accuracy and robust performance in anomaly detection when compared with the approaches using raw monitoring data.

Acknowledgements

The research reported in this paper was supported in part by the National Natural Science Foundation of China under Grant No. 51208096, the Key Science and Technology Project of Jiangsu Transport Department, China under Grant No. 2014Y02 and No. 2019Z02, the Natural Science Foundation of Jiangsu Province under Grant No. BK20181278 and China Postdoctoral Science Foundation under Grant No. 2019M653085. The authors thank the anonymous reviewers for their constructive comments and advice, which greatly improved the quality of this manuscript.

References

[1] Xu X, Huang Q, Ren Y, Zhao D, Zhang D and Sun H 2019 Condition evaluation of suspension bridges for maintenance, repair and rehabilitation: a comprehensive framework *Struct. Infrastruct. E.* **15** 555-67.

[2] Zhou G, Yi T, Xie M and Li H 2017 Wireless sensor placement for structural monitoring using information-fusing firefly algorithm *Smart Mater. Struct.* **26** 104002.

[3] Wang W, Jiang S, Zhou H, Yang M, Ni Y and Ko J 2018 Time synchronization for acceleration measurement data of Jiangyin Bridge subjected to a ship collision *Struct. Control Hlth. Monit.* **25** e2039.

[4] Xiong W, Cai C S, Kong B, Zhang X and Tang P 2019 Bridge scour identification and field application based on ambient vibration measurements of superstructures *J. Mar. Sci. Eng*. **7** 121-44.

[5] Lin TK, Wu RT, Chang KC and Chang YS 2013 Evaluation of bridge instability caused by dynamic scour based on fractal theory *Smart Mater. Struct.* **22** 075003.

[6] Ying Z, Ni Y and Kang L 2019 Modal localization characteristics of damaged quasi-periodically supported beam structures with local weak coupling *Struct. Control Hlth. Monit.* **26** e2351.

[7] Hao S 2009 I-35W bridge collapse *J. Bridge Eng.* **15** 608-614.

[8] Xu X, Huang Q, Ren Y, Zhao D and Yang J 2019 Sensor fault diagnosis for bridge monitoring system using similarity of symmetric responses *Smart Struct. Syst.* **23** 279-93.

[9] Huang Y, Shao C, Wu S and Li H 2019 Diagnosis and accuracy enhancement of compressive-sensing signal reconstruction in structural health monitoring using multi-task sparse Bayesian learning *Smart Mater. Struct.* **28** 035001.

[10] Liu B, Do P, Iung B, and Xie M 2019 Stochastic filtering approach for condition-based maintenance considering sensor degradation *IEEE Autom. Sci. and Eng*. online.

[11] Liu Y, Liu B, Zhao X, and Xie M 2018 Development of RVM-based multiple-output soft sensors with serial and parallel stacking strategies *IEEE T. Contr. Syst. T*. **27** 2727-2734.
[12] Zhang Z, Sun C, Li C and Sun M 2019 Vibration based bridge scour evaluation: A data-driven method using support vector machines *Struct. Monit. Maint*. **6** 125-45.
[13] Zhou X, Ni Y and Zhang F 2014 Damage localization of cable-supported bridges using modal frequency data and probabilistic neural network *Math. Probl. Eng*. **2014** 837963.
[14] Yan Y, Cheng L, Wu Z and Yam L H 2007 Development in vibration-based structural damage detection technique *Mech. Sys. Signal Pr*. **21** 2198-211.
[15] Salawu O S 1997 Detection of structural damage through changes in frequency: a review *Eng. Struct.* **19** 718-23.
[16] Tatar A, Niousha A and Rofooei F R 2017 Damage detection in existing reinforced concrete building using forced vibration test based on mode shape data *J. Civil Struct. Hlth Monit.* **7** 123-35.
[17] Hoell S and Omenzetter P 2018 Sequential projection pursuit for optimized vibration-based damage detection in an experimental wind turbine blade *Smart Mater. Struct*. **27** 025007.
[18] Ko J, Ni Y, Wang J, Sun Z and Zhou X 2000 Studies of vibration-based damage detection of three cable-supported bridges in Hong Kong *Proc. of the Int. Conf. on Engineering and Technological Science 2000*.
[19] Wang B, Ni Y and Ko J M 2011 Damage detection utilising the artificial neural network methods to a benchmark structure *Int. J. Struct. Eng*. **2** 229-42.
[20] Yam L H, Yan Y J and Jiang J S 2003 Vibration-based damage detection for composite structures using wavelet transform and neural network identification *Compos. Struct*. **60** 403-12.
[21] Zhou J, Fan Z and Feng X 2013 A novel transmissibility concept based on wavelet transform for structural damage detection. *Smart Struct. Syst.* **12** 291-308.
[22] Wang J and Ni Y 2015 Refinement of damage identification capability of neural network techniques in application to a suspension bridge *Struct. Monit. Maint*. **2** 77-93.
[23] Lu W, Teng J, Xu Y and Su Z 2013 Identification of damage in dome-like structures using hybrid sensor measurements and artificial neural networks *Smart Mater. Struct*. **22** 105014.
[24] Cross E J, Worden K, and Chen Q 2011 Cointegration: a novel approach for the removal of environmental trends in structural health monitoring data *P. Roy. Soc. A – Math. Phy.* **467** 2712-32.
[25] Xu Z and Wu Z 2007 Simulation of the effect of temperature variation on damage detection in a long-span cable-stayed bridge *Struct. Hlth. Monit.* **6** 177-89.
[26] Peeters B, Maeck J and Roeck G D 2001 Vibration-based damage detection in civil engineering: excitation sources and temperature effects *Smart Mater. Struct*. **10** 518-27.
[27] Posenato D, Kripakaran P, Inaudi D, and Smith I F 2010 Methodologies for model-free data interpretation of civil engineering structures *Comput. Struct.* **88** 467-482.
[28] Wu B, Wu G, Yang C and He Y 2018 Damage identification method for continuous girder bridges based on spatially-distributed long-gauge strain sensing under moving loads *Mech. Sys. Signal Pr*. **104** 415-35.
[29] Chen C, Wu W, Liu C and Lai G 2016 Damage detection of a cable-stayed bridge based on the variation of stay cable forces eliminating environmental temperature effects *Smart Struct. Syst*. **17** 859-80.
[30] Yu Z, Xia H, Goicolea J M and Xia C 2016 Bridge damage identification from moving load induced deflection based on wavelet transform and Lipschitz exponent *Int. J. Struct. Stab. Dy*. **16** 1550003.
[31] Zhu Y, Ni Y, Jin H, Inaudi D and Laory I 2019 A temperature-driven MPCA method for structural anomaly detection *Eng. Struct.* **190** 447-58.

[32] Yarnold M T, and Moon F L 2015 Temperature-based structural health monitoring baseline for long-span bridges *Eng. Struct*. **86** 157-167.
[33] Kromanis R, and Kripakaran P 2014 Predicting thermal response of bridges using regression models derived from measurement histories *Comput. Struct*. **136** 64-77.
[34] Zhu Y, Ni Y, Jesus A, Liu J and Laory I 2018 Thermal strain extraction methodologies for bridge structural condition assessment *Smart Mater. Struct*. **27** 105051.
[35] Xu X, Huang Q, Ren Y, Zhao D, Yang J and Zhang D 2019 Modeling and separation of thermal effects from cable-stayed bridge response *J. Bridge Eng*. **24** 04019028.
[36] Ren Y, Xu X, Huang Q, Zhao D and Yang J 2019 Long-term condition evaluation for stay cable systems using dead load-induced cable forces *Adv. Struct. Eng*. **22** 1644-56.
[37] Zong Z, Zhong R, Zheng P, Qin Z and Liu Q 2014 Damage and safety prognosis of bridges structures based on structural health monitoring: progress and challenge *China J. Highway Transp.* **27** 46-57.
[38] Chandola V, Banerjee A and Kumar V 2009 Anomaly detection: a survey *ACM Comput. Surv*. **41** 1-58.
[39] Qin Z, Chen L and Bao X 2012 Wavelet denoising method for improving detection performance of distributed vibration sensor. *IEEE Photonic. Tech. L.* **24** 542-44.
[40] Ding Y, Li A and Deng Y 2010 Structural damage warning of a long-span cable-stayed bridge using novelty detection technique based on wavelet packet analysis *Adv. Struct. Eng*. **13** 291-8.
[41] Zhou Y, Sun L and Peng Z 2015 Mechanisms of thermally induced deflection of a long-span cable-stayed bridge *Smart Struct. Syst*. **15** 505-22.
[42] Su J, Xia Y, Ni Y, Zhou L and Su C 2017 Field monitoring and numerical simulation of the thermal actions of a supertall structure *Struct. Control Hlth Monit*. **24** e1900.
[43] Hu Y, Xia Q, Xia Y and Hou R 2019 Temperature-induced displacement of supertall structures: a case study *Adv. Struct. Eng*. **22** 982-96.
[44] Zhao D, Huang Q, Ren Y and Xu X 2019 Analysis of temperature-induced deflection of cable-stayed bridge based on BP neural network *IOP Conf. Series Earth and Environmental Science* **242** 062075.
[45] Ding Y, Li A, Sun J and Deng Y 2009 Research on seasonal correlation of wavelet packet energy spectrum and temperature of Runyang Suspension Bridge *Sci. China Ser. E-Technol. Sci.* **52** 1776-85.
[46] Kromanis R and Kripakaran P 2017 Data-driven approaches for measurement interpretation: analysing integrated thermal and vehicular response in bridge structural health monitoring *Adv. Eng. Inform.* **34** 46-59.
[47] Liu Y, Deng Y and Cai CS 2015 Deflection monitoring and assessment for a suspension bridge using a connected pipe system: a case study in China *Struct. Control Hlth. Monit*. **22** 1408-25.
[48] Deng Y, Li A, Liu Y and Chen S 2018 Investigation of temperature actions on flat steel box girders of long-span bridges with temperature monitoring data *Adv. Struct. Eng*. **21** 2099-113.
[49] Jung J, Kim DJ, Vadivel SKP and Yun SH 2019 Long-term deflection monitoring for bridges using X and C-band time-series SAR interferometry *Remote Sens*. **11** 1258.
[50] Deng Y, Li A, Chen S and Feng D 2018 Serviceability assessment for long-span suspension bridge based on deflection measurements *Struct. Control Hlth. Monit.* **25** e2254.
[51] Xu YL, Chen B, Ng CL, Wong KY and Chan WY 2010 Monitoring temperature effect on a long suspension bridge *Struct. Control Hlth. Monit.* **17** 632-53.
[52] Xia Q, Zhang J, Tian Y, and Zhang Y 2017 Experimental study of thermal effects on a long-span suspension bridge *J. Bridge Eng.* **22** 04017034

[53] Zhou Y and Sun L 2019 Insights into temperature effects on structural deformation of a cable-stayed bridge based on structural health monitoring *Struct. Heal. Monit.* **18** 778-91.